Neurobiology of Disease 132 (2019) 104568

Contents lists available at ScienceDirect

Neurobiology of Disease

journal homepage: www.elsevier.com/locate/ynbdi

Glucocorticoid receptors modulate dendritic spine plasticity and microglia activity in an animal model of Alzheimer's disease

Matteo Pedrazzoli[a], Morris Losurdo[b], Giovanna Paolone[c], Manuela Medelin[a], Lejdi Jaupaj[a], Barbara Cisterna[a], Anna Slanzi[d], Manuela Malatesta[a], Silvia Coco[b], Mario Buffelli[a,*]

[a] University of Verona, Department of Neurosciences, Biomedicine and Movement Sciences, Verona, Italy
[b] University of Milano-Bicocca, School of Medicine and Surgery, Milan, Italy
[c] University of Verona, Department of Diagnostics and Public Health, Verona, Italy
[d] University of Verona, Department of Medicine, Verona, Italy

ARTICLE INFO

Keywords:
Glucocorticoid receptor
Glucocorticoids
Hippocampus
Microglia
Dendritic spines
Alzheimer's disease

ABSTRACT

Chronic exposure to high circulating levels of glucocorticoids (GCs) may be a key risk factor for Alzheimer's Disease (AD) development and progression. In addition, hyper-activation of glucocorticoid receptors (GRs) induces brain alterations comparable to those produced by AD. In transgenic mouse models of AD, GCs increase the production of the most important and typical hallmarks of this dementia such as: Aβ40, Aβ42 and tau protein (both the total tau and its hyperphosphorylated isoforms). Moreover, GCs in brain are pivotal regulators of dendritic spine turnover and microglia activity, two phenomena strongly altered in AD. Although it is well-established that GCs primes the neuroinflammatory response in the brain to some stimuli, it is unknown whether or how GRs modulates dendritic spine plasticity and microglia activity in AD. In this study, we evaluated, using combined Golgi Cox and immunofluorescence techniques, the role of GR agonists and antagonists on dendritic spine plasticity and microglia activation in hippocampus of 3xTg-AD mice. We found that dexamethasone, an agonist of GRs, was able to significantly reduce dendritic spine density and induced proliferation and activation of microglia in CA1 region of hippocampus of 3xTg-AD mice at 6 and 10 months of age. On the contrary, the treatment with mifepristone, an antagonist of GRs, strongly enhanced dendritic spine density, decreased microglia density and improved the behavioural performance of 3xTg-AD mice. Additionally, primary microglial cells *in vitro* were directly activated by dexamethasone. Together, these data demonstrate that stress exacerbates AD and promotes a rapid progression of the pathology acting on both neurons and glial cells, supporting an important pro-inflammatory role of GC within CNS in AD. Consequently, these results further strengthen the need to test clinical interventions that correct GCs dysregulation as promising therapeutic strategy to delay the onset and slow down the progression of AD.

1. Introduction

Alzheimer's disease (AD), the most common form of dementia in the elderly, is characterized by dramatic synaptic degeneration and neuronal death, leading to memory impairment (Bolognin et al., 2014; De Strooper and Karran, 2016; Serrano-Pozo et al., 2011).

Many pathophysiological mechanisms have been proposed to cause synaptic dysfunction and dendritic atrophy in AD, including accumulation of amyloid beta (Aβ), hyperphosphorylation of tau proteins in neurons, Rac1 deregulation, inflammation and altered levels of circulating glucocorticoids (Borin et al., 2018; Canet et al., 2018; Dorostkar et al., 2015; Ferreira et al., 2015; Kootar et al., 2018; Sala and Segal, 2014; Ziegler-Waldkirch and Meyer-Luehmann, 2018).

Glucocorticoids (GCs) are a class of steroid hormones that act on brain, through mineralcorticoid (MRs) and glucocorticoid receptors (GRs), regulating physiological and behavioural responses under baseline conditions and after stress. The production of GCs is finely controlled by the hypothalamic-pituitary-adrenal (HPA) axis, a complex neuroendocrine system that involves the paraventricular nucleus of hypothalamus (PVN), the pituitary gland and the adrenal cortex. High and chronic circulating levels of GCs in blood, may be a symptom of a dysfunction of the HPA axis, and are typically observed in diseases such as chronic stress (Finsterwald and Alberini, 2014), depression (Dienes et al., 2013), and AD (Csernansky et al., 2006; Pietrzak et al., 2017;

* Corresponding author at: Department of Neurosciences, Biomedicine and Movement Sciences, University of Verona, Strada le Grazie, 8, 37131 Verona, Italy.
E-mail address: mario.buffelli@univr.it (M. Buffelli).

https://doi.org/10.1016/j.nbd.2019.104568
Received 9 April 2019; Received in revised form 24 July 2019; Accepted 2 August 2019
Available online 05 August 2019
0969-9961/

Swaab et al., 1994; Umegaki et al., 2000).

Studies in human and in mice have shown that chronic exposure to GCs and chronic stress paradigms induce proinflammatory and neurotoxic cytokines in several regions in the brain (Duque Ede and Munhoz, 2016; Munhoz et al., 2006; Munhoz et al., 2010; Sorrells et al., 2009), degeneration of dendritic spines in hippocampus and prefrontal cortex (Liston and Gan, 2011; Magarinos et al., 1996), impairment of hippocampal neurogenesis (Lemaire et al., 2000; Mirescu et al., 2006) and behaviour (Hammar and Ardal, 2009; Wilson et al., 2005). Lastly, in models of familial AD, chronic stress and exogenous GCs increased the production of Aβ40, Aβ42 and Tau (Carroll et al., 2011; Dong et al., 2008; Green et al., 2006; Joshi et al., 2012), other known contributors to AD pathophysiology. Moreover, it is known that a rare haplotype of *hsd11b1* gene, that codifies for a cortisone reductase, is associated with a 6-fold increased risk for sporadic AD (de Quervain et al., 2004) underlining the existence of a correlation between GCs and AD. Together, these data suggest a strong correlation between blood levels of GCs and neuropathological alterations typical of AD.

Even though AD is primarily a neuronal disease, microglia disfunction has recently been implicated in virtually every neurodegenerative disorder, including AD (Mcquade and Blurton-Jones, 2019; Wang and Colonna, 2019). Microglia are the resident immune cells of the central nervous system (CNS) that exert important roles in the maintenance of CNS homeostasis and remodelling of neuronal circuits across development and experience-dependent plasticity (Paolicelli and Ferretti, 2017). Several lines of evidence show that microglial response play an important role in linking the effects of chronic stress with the onset and progression of AD (Bisht et al., 2018; Piirainen et al., 2017). In particular, microglia express GRs (Sierra et al., 2008) and long-lasting high circulating levels of GCs are able to induce a pro-inflammatory response in the brain with changes in microglial ramification, proliferation and activation of microglia in the brain (Frank et al., 2014; Nair and Bonneau, 2006; van Olst et al., 2018).

However, the role of GRs activity on dendritic spine plasticity and microglia in AD mouse models is still under debate. Here, we verify whether GRs modulation could interfere, positively or negatively, with dendritic spine plasticity in CA1 region of 3xTg-AD mice, the triple transgenic model for AD (Belfiore et al., 2019; Oddo et al., 2003). Moreover, we analyse whether the spine loss due to GCs is mediated by activation of microglial cells. We found that an agonist of GRs was able to decrease dendritic spine density and induced proliferation and activation of microglia in CA1 region of hippocampus of 3xTg-AD mice, while an antagonist of GRs strongly enhanced dendritic spine density and improved the behavioural performance of 3xTg-AD mice.

2. Materials and methods

2.1. Animal treatment

We used 3xTg-AD mice expressing three mutant human transgenes—PS1 (M146V), βAPP (Swedish) and tau (P301L)24 that were purchased from The Jackson Laboratory (Sacramento, CA) (Belfiore et al., 2019; Oddo et al., 2003). Although the 3xTg-AD mice were originally derived from a 129/C57BL6 background, genetic analysis showed that our 3xTg-AD mouse colony matched ~80% of the allelic profiles of C57BL/6 mice after ten generations of random mating. All experiments were performed in accordance with the EU guidelines (2010/63/UE) and Italian law (decree 26/14) and were approved by the local authority veterinary service and by our university ethical committee. All efforts were made to minimize animal suffering and to reduce the number of animals used. Animal use was approved by the Italian Ministry of Health, in agreement with the EU Recommendation 2007/526/CE. In particular, in the results for Golgi Cox staining, for the combined technique of Golgi Cox and immunofluorescence experiments and for the electron microscopy analyses, the number of animals were 4 per each condition (3xTg-AD vehicle, 3xTg-AD dexamethasone and 3xTg-AD mifepristone). While, for behavioural tests the mice tested were 8 per group (wild-type, 3xTg-AD vehicle, 3xTg-AD dexamethasone, 3xTg-AD mifepristone), for a total of 32 mice at 6 months of age and 10 months of age.

6 and 10 months old 3xTg-AD male mice were treated with the GRs agonist, dexamethasone (D4902 Sigma-Aldrich), or the GR antagonist, mifepristone (M8046 Sigma-Aldrich), or only vehicle through intraperitoneal injections (i.p., four animals per group). It is well-known that in 3xTg-AD there are several sex differences (Oddo et al., 2003), but we were forced to use only males to reduce the side effects of mifepristone linked to inactivation of progesterone receptors in females. Injections were performed for 5 consecutive days at 11 o'clock to not interfere with glucocorticoid circadian rhythm. Dexamethasone and mifepristone stock solutions were prepared using DMSO, at 20 mg/ml and 5 mg/ml, respectively. The day of the injection the stock solution was diluted in 10% Tween-20 plus distilled water to obtain a dexamethasone concentration of 8 mg/Kg and a mifepristone concentration of 20 mg/kg. These doses of drugs are comparable with those used in literature (Liston and Gan, 2011). Three days after the last injection, animals were used for behavioural test or anesthetized using Tribromoethanol (TBE) drug, and perfused transcardially with 0.1 M phosphate buffer solution (PBS) followed by formaldehyde 10% V/V, buffered 4% W/V (Titolchimica-Italy), for imaging studies; finally, brains were extracted and postfixed overnight.

2.2. Golgi cox staining

The day after, brains were transferred in 200 ml of Golgi Cox solution at dark for 2 weeks. The Golgi Cox solution contains 1% Mercury Chloride, 1% Potassium Dichromate and 1% Potassium Chromate in distilled water (Das et al., 2013; Zaqout and Kaindl, 2016). After the staining, brains were left in 30% Sucrose solution (in PBS) for 24 h to reduce the tissue fragility for the next cut (Gibb and Kolb, 1998). Then, 100 μm thick slices were collected using vibratome (Leica VT1200, Leica Biosystems, Germany) and were passed in Kodak Developer and Fixer for 5 and 15 min, respectively, and washed in distilled water for 5 min after each step. Finally, slices were dehydrated using increasing concentrations of Ethanol (50%–60%–75%–85%). To avoid slices fragmentation, the dehydration did not reach 100%. At the end, slices were mounted on slides using Eukitt (Sigma Eldrich, USA).

2.3. Brightfield microscopy and dendrite analysis

Images were collected using Olympus BX63 microscope (Olympus Corporation, Japan) and acquired by Neurolucida 64-Bit software (MBF Bioscience, USA). Acquisition of dendritic spines in CA1 region of hippocampus occurred at 100x. We collected images of 117 × 88 μm and analysed three slices per mice between −1.955 mm and −2.355 mm Bregma. Every stack was acquired using a z-step size of 0.35 μm. Images were deconvolved through AutoQuant software, converted in 8bit images and, then, black signal was inverted to allow the analyses with Imaris-Bitplane Software.

Neuronal dendrites and spines in the CA1 region were reconstructed using Autopath system of Imaris. Every single spine detected by the Software was manually checked to avoid false positive signals. At that point, Imaris gave us information about the dendritic length and the number of spines. To reduce the bias related to different dendrite lengths, we calculated the medium spine density for each animal dividing the total number of spines with the total length of every dendrite.

2.4. Combined Golgi cox and immunofluorescence tecnique

6 and 10 months old 3xTg-AD male mice were treated with Dexamethasone or only vehicle by using the same method exposed above (four animals per group). After the perfusion and the overnight

post-fixation, each mouse brain was transferred in Golgi Cox solution for 2 weeks. Then, brains were cut and slices were immersed in PBS into a 24 well plate and treated with Kodak Developer and Fixer. At that point we stopped the Golgi protocol and proceeded with the immunofluorescence staining (modified by (Spiga et al., 2011). We treated slices for 30 min with the blocking solution, composed of 3% Bovine Serum and 0.3% triton in PBS. After we stained slices with primary IBA1 antibody (WAKO-1:500) to mark microglia activation and proliferation. The staining lasts for 36 h at 4 °C, at dark. Then we proceeded with secondary antibody staining for 2 h. Finally, we treated slices with 0.2% DAPI solution in PBS and slices were mounted on Xtra slides using Para Phenylenediamine (PPD).

2.5. Confocal microscopy and image analysis

Images were acquired using Leica-Sp5 Confocal Microscopy. 20x magnification was used to detect microglial cells for the density analyses; glycerol 63X objective was used to acquire images for morphological analyses of microglia. Bright-field signal of Golgi-stained neurons was detected through confocal reflection microscopy, while microglia fluorescent signal was detected, simultaneously, through confocal fluorescent microscopy. We collected a total stack thickness of 50 μm (z-step size = 0.5 μm) for a total volume of 0.0144 mm^3. Dendrites and spines of CA1 neurons were reconstructed using the "Filaments" Autopath system of Imaris 9.1 software (Bitplane, Zurich, Switzerland). Microglial cells were 3D rebuilt through the "Cell" function system of Imaris, taking advantage of the threshold that allowed us to reconstruct the whole visible cells. For each mouse, the microglia density was calculated dividing the total number of cells, counted using ImageJ, with the volume of slice. Area and volume were calculated directly by "cell analysis" function of Imaris.

In order to quantify the percentage of microglia in contact with neurons, the morphology of the Golgi labeled neurons, including their processes, were 3D reconstructed from image stacks with the Imaris and subsequently assessed by MatLab R2014b software (MCR v8.3 Mathworks, Natick, MA, USA). Creation of solid isosurface matching the fluorescent signal was based on absolute intensity for the Golgi positive neurons and processes *via* a threshold-based segmentation algorithm.

Concerning the microglial cells labeled with Iba1, the size of the processes was also taken in account. In particular, a minimum diameter of 1 μm was determined by using the line tool (slice view mode) to measure the diameter of the thinnest process signal in the confocal stack. Moreover, the background subtraction was enabled and the interactive software histogram of the fluorescent signal quality was used to select a threshold to include as much as possible of the microglial cells signal, while excluding the background. Spots were created based on the microglia signal and the threshold choice was set at an appropriate value, which covers all the microglia fluorescent signal. MatLab's plugin on Imaris made possible the isolation of the microglia spots to a selected distance from the Golgi 3D surface. The percentage of microglia signal close to neurons was calculated by dividing the number of microglia spots closer than 10 μm and 1 μm to the neurons over the total number of microglia spots in a confocal volume.

2.6. Electron microscopy

For the ultrastructural analysis, 4 Vehicle and 4 Mifepristone 3xTg-AD 6 months-old mice were perfused with 2% formalin and 2.5% glutaraldehyde in phosphate buffer pH 7.4. The brain was then excised, fixed in 2% paraformaldehyde and 2.5% glutaraldehyde in phosphate buffer pH 7.4 for 3 h at 4 °C, washed in PBS and sectioned in slices of 40 μm. The slices were then post-fixed with 1% OsO4 for 2 h at 4 °C and dehydrated with acetone. CA1 region was cut out and embedded in Epon resin. Ultrathin sections were observed with a Philips Morgagni transmission electron microscope (FEI Company Italia Srl), operating at 80 kV and equipped with a Megaview III camera for digital image acquisition and analysis. For morphometrical evaluation, ten images of longitudinally sectioned dendrites were taken at a fixed magnification (14,000×) per animal.

The index of dendritic membrane irregularity (expressed as the ratio between the real length of the membrane profile and the corresponding linear length) and the density of spines with or without pre-synaptic terminal (the ratio between spine number and linear length) were assessed by using ImageJ software. The synaptic contact was identified by the presence of both the pre-synaptic element containing the typical vesicles and the post-synaptic electrondensity.

2.7. Behavioural test

3xTg-AD mice (n = 8 per group), together with C57BL/6 mice (n = 8) for wild-type controls, were tested with Open field arena and Y-Maze test. The effects of vehicle, dexamethasone and mifepristone on locomotor activity and spatial learning and memory capabilities were investigated using the open field arena (OF, Open Field Cages, Ugo Basile, Varese, Italy) and the Y-Maze test (Y-Maze System for mice, Ugo Basile, Varese, Italy), respectively. Each test was performed at 6 and 10 months of age. Prior to treatment, 3xTg-AD mice were randomly assigned to the 3 groups: vehicle, dexamethasone, and mifepristone. For the OF test, mice were placed in center of the arena (44 × 44 × 30 cm) and video-monitored for 20 min. Video were analysed (AnyMaze) for distance moved, immobility, entries and time spent in the center part of the arena.

For the Y-Maze test, each mouse was placed in the center of a symmetrical Y-maze with the three arms arranged at 120°to each other. Mice were allowed to freely explore the maze for 8 min and the total number of transitions and the sequence of arms entered were recorded. Alternation was defined as successive entries into the three arms in overlapping triple sets. To reduce odor cues, the maze was cleaned with 10% ethanol solution after each session. Experimenters were blinded with respect to the mice treatment.

2.8. Microglial cell culture

Primary cultures of microglial cells were isolated from mixed cultures of cortical and hippocampal astrocytes, established from brains of postnatal 1–2 days old C57BL/6 mice.

Briefly, after the removal of meninges, cortices and hippocampi were isolated and subjected to mechanical digestion. The obtained cell suspension was filtered with 70 μm nytex membrane, centrifuged 10 min at 800 ×*g* at RT and finally resuspended in complete glial medium [Eagle's minimal essential medium (MEM, Gibco®)], 20% fetal bovine serum (Sigma-Aldrich), 33 mM Glucose (Sigma-Aldrich), 1% Na-Pyruvate (Lonza), 2 mM L-ultra glutamine, 100 μg/ml streptomycin and 100 U/ml penicillin (all from Euroclone)].

After about 14 days microglial cells were harvested by shaking the flasks at 230 rpm for 45 min at RT and seeded at a concentration of about 2×10^5 cells on 24 mm plate wells, previously pre-coated with 0.05 mg/ml poly-Ornithine (Sigma-Aldrich) for western blot analysis (WB). For immunofluorescence, microglia were plated at a concentration of about 8×10^4 cells on 18 mm glass coverslips, pre-coated with poly-Ornithine as previously described for plate wells. To minimize activation, microglia cells were grown in a medium consisting from 5/6 glial medium without serum and 1/6 astrocyte-conditioned 0.22 um filtered medium.

Microglial cells were plated for 24 h before being exposed to GRs agonist and antagonist drugs [dexamethasone (1 μM), diluted in DMSO and PBS, and mifepristone (1 μM), diluted in DMSO] for 4 h. Cultures treated only with vehicle were used as control.

Afterwards, medium was removed, and cells were lysed for WB analysis or fixed for immunofluorescence processing.

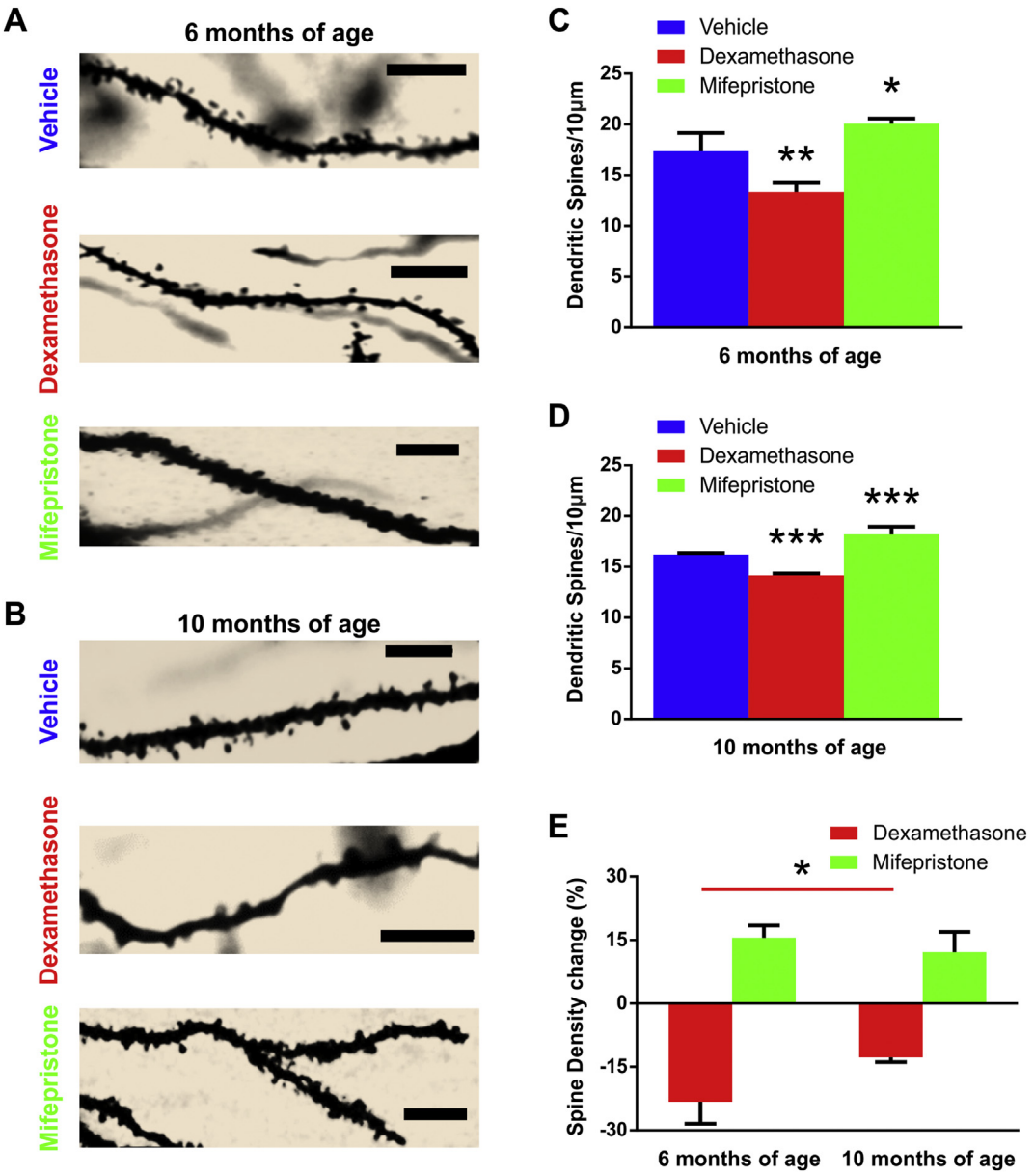

Fig. 1. Dexamethasone and mifepristone differently modulate dendrite spine density. (A-B) Representative images of dendrites labeled with Golgi Staining in hippocampal CA1 of vehicle, dexamethasone and mifepristone treated 3xTg-AD mice at 6 (A) and 10 (B) months of age. (C-D) Bar graphs showing the dendritic spine density in all the conditions (vehicle, dexamethasone and mifepristone treated 3xTg-AD mice, at 6 and 10 months of age). (E) Bar graphs showing that Dexamethasone-induced reduction of dendritic spine density was stronger at 6 months, while the Mifepristone-induced increase of dendritic spines density was similar at 6 and 10 months of age. Significant differences are indicated as follows: *p < 0.05, **p < 0.01, ***p < 0.001. Scale bars = 5 µm.

2.9. Immunofluorescence of microglial cell culture

After fixation, microglial cells were treated for immunofluorescence experiments to label nuclei (DAPI) and cells with a microglia marker (IBA1) and a marker of M1 pro-inflammatory state (CD68). In detailed, the protocol was similar to that previously described, but with different timing.

Cells were permeabilized and blocked in 3% Bovine Serum and 0.3% triton in PBS for 15 min at room temperature (RT). Afterwards, cells were incubated with primary Rabbit IBA1 antibody (WAKO-1:500) and Rat CD68 antibody (Biorad–1:200), diluted in the blocking solution overnight at 4 °C. Upon washing, cells were then incubated with secondary antibodies: Donkey Anti-Rabbit Alexa Fluor 488 (Invitrogen–Thermofisher, 1:1000) and Donkey Anti-Rat Alexa Fluor 594 (Invitrogen–Thermofisher, 1:1000) both diluted in the blocking solution, for 1 h at RT. After 3 washes with PBS we labeled nuceli with DAPI (1:2000 in PBS) for 5 min at RT. Finally, coverslips were mounted on Xtra slides using Para Phenylenediamine (PPD).

2.10. Western blot analyses

Microglia cells were lysed for the analysis of specific markers by WB. Cell phenotype was investigated by the following antibodies: rat monoclonal anti-CD68 (1:400, Biorad, Hercules, CA, USA), rat monoclonal anti- CD206 (1:400, Biorad, Hercules, CA, USA). Total protein amount was evaluated by means of bicinchoninic acid assay. 15 µg of each sample were subjected to SDS-polyacrylamide gel electrophoresis and transferred to a nitrocellulose membrane (GE Healthcare). All the data were normalized to β-actin (1:1000, Sigma-Aldrich).

CD68 and CD206 microglia markers were investigated in non-reducing conditions, as specified by manufacturer's instructions. At this aim, protein samples were prepared in loading buffer composed by 8%

sodium dodecyl sulphate (SDS), 40% glycerol, 0.004% bromophenol blue, 0.2 M Tris-HCl, (pH 6.8).

Blocking and antibody probing occurred in TBS-Tween 0.1% buffer containing 5% non-fat milk. Secondary anti-rat antibodies (1:5000, *Genetex, Irvine, CA, USA*) were used for detection of rat anti-mouse CD68 and CD206 antibodies. Immunoblot band chemiluminescence was analysed and semi-quantified by ImageQuant™ LAS 4000 (*GE Healthcare Life Sciences*).

2.11. Statistical analyses

Results are presented as mean ± standard deviation (SD). One way Anova and two way Anova (in Fig. 4 Treatment and Age as factors; in Fig. 5 Treatment and Distance from neurons as factors) were used when multiple groups were compared, with post-hoc analysis performed by Tukey's test. A statistically significant difference between two data sets was assessed by Student's *t*-test. In every experiment, an alpha of 0.05 was used as the cutoff for significance.

3. Results

3.1. Glucocorticoid receptor modulation significantly altered dendritic spine density of neurons in the ca1 region of hippocampus

Loss of dendritic spines is a common alteration of AD (Bolognin et al., 2014; Scheff et al., 2007), but it has never been described before in untreated 3xTg-AD mice younger than 10 months of age (Belfiore et al., 2019; Bittner et al., 2010; Oddo et al., 2003). To verify whether the activity of GRs modulates positively and/or negatively the dendritic spine plasticity in this animal model of AD, we administered 8 mg/kg of dexamethasone (i.p.) or 20 mg/kg of mifepristone or only vehicle to 3xTg-AD mice at 6 and 10 months of age.

Our results show that 5 days of treatment with the GRs agonist promoted a strong reduction of the dendritic spine density in the CA1 region of the hippocampus of about 23% at 6 months of age (dendritic spines/10 μm = 17.37 ± 1.79 and 13.34 ± 0.90 for vehicle and dexamethasone, respectively; $F(2,10) = 28.62$, $p < 0.01$) and 12.7% at 10 months of age (dendritic spines/10 μm = 16.23 ± 0.14 and 14.16 ± 0.18 for vehicle and dexamethasone, respectively; $F(2,9) = 74.91$, $p < 0.001$; Fig. 1). In addition, based on a qualitative observation of the dendritic arborization, dexamethasone was also able to induce atrophy of the dendritic trees, a neuropathological hallmark of AD, that has never been observed in this animal model (Belfiore et al., 2019; Oddo et al., 2003; Wirths and Bayer, 2010). Indeed, in 3xTg-AD mice, the only impairment at the functional level at early stages of the disease, is the LongTerm Potentiation dysfunction in hippocampus (Bertoni-Freddari et al., 2008; Oddo et al., 2003).

It is noteworthy that the effects of GRs agonist were stronger at the beginning of the pathology (6 months of age) rather than in the middle late phase (10 months of age) ($p < 0.05$, Fig. 1E).

On the contrary, the administration of mifepristone, a GRs antagonist, induced an increase of dendritic spine density of about 15.5% (Vehicle: 17.37 ± 1.6; Mifepristone: 20.06 ± 0.516; $p < 0.05$) and 12.1% (Vehicle: 17.37 ± 1.6; Mifepristone: 18.20 ± 0.78; $p < 0.001$), at 6 and 10 months of age, respectively (Fig. 1). These data are in contrast with those previously published in mifepristone-treated rodents where the blockade of GRs reduced the formation of dendritic spines (Liston and Gan, 2011). However, our results could explain the behavioural improvements found in two AD mice models treated with mifepristone (Baglietto-Vargas et al., 2013; Lante et al., 2015).

At the ultrastructural level, we observed an evident increase in the irregularity of the dendritic membrane in mifepristone-treated 3xTg-AD mice at 6 months of age (Fig. 2A, pink). The irregularity index was, in fact, significantly higher in the mifepristone-treated samples ($p < 0.05$) and could be linked to the process of spine formation. The density of dendritic spines without synaptic contact significantly increased in mice treated with mifepristone in comparison to vehicle ($p < 0.05$, Fig. 2B), strongly supporting the result obtained with the Golgi-Cox Staining. Conversely, the density of dendritic spines with synaptic contact seemed to be similar in the two experimental groups ($p = 0.65$, Fig. 2B). Finally, we were able to find few perforated synapses in 3xTg-AD mifepristone-treated mice, but no perforated synapses have been detected in control mice. Consequently, we suggested that mifepristone could increase the number of perforated synapses whose decline represents the only impairment related to spines observed in 3xTg-AD mice at the beginning of the disease (Bertoni-Freddari et al., 2008; Stewart et al., 2005).

3.2. Glucocorticoid receptors modulation alter open field arena and y-maze test performance in 3xtg-ad mice

It has been shown that in 12 months old 3xTg-AD mice, mifepristone treatment rescues the pathologically induced cognitive impairments and markedly reduces Aβ and tau pathologies (Baglietto-Vargas et al., 2013). Here, to verify whether GRs agonist and antagonist could affect 3xTg-AD mice behaviour at 6 and 10 months of age, we performed the open field and the Y-maze tests in treated (3xTg-AD) and wild-type mice C57BL/6.

As expected, the distance travelled, as measured in the open maze test, decreased over time in all experimental groups compared to WT mice (main effect of time: $F(1,28) = 22.46$, $p < 0.001$; Fig. 3A). In addition, ANOVA analysis revealed a significant interaction between time and treatment (time x treatment: $F(3,28) = 4.89$, $p < 0.05$). However, more detailed analyses showed that 3xTg-AD mice motor functions were not affected by any of the drug treatments. Similar patterns were observed at both time points (main effect of genotype, 6 months: $F(1,31) = 94.22$, $p < 0.001$; 10 months: $F(1,31) = 56.44$, $p < 0.001$). Conversely, spatial learning memory performance, evaluated by the Y maze test, was affected by time, (main effect of time $F(1,2) = 11.24$, $p < 0.01$), with the ANOVA also revealing a main effect of the treatment ($F(3,27) = 16.85$, $p < 0.001$). In fact, although 3xTg-AD mice performed significantly worse than WT ones at both ages, the performance of transgenic animals treated with mifepristone resulted significantly higher, compared to vehicle treated mice, only at 10 months and was comparable to the level of performance exhibited at 6 months of age (Fig. 3B).

3.3. Dexamethasone increased microglia density and activation in ca1 region of hippocampus

Many mechanisms could induce dendritic atrophy in AD (Bittner et al., 2010; Borin et al., 2018; Dorostkar et al., 2015). To check whether dendritic spine degeneration induced by dexamethasone is mediated by activation of microglia, we analysed microglia density and morphology in vehicle- and dexamethasone-treated 3xTg-AD mice. We found that drug administration increased microglia density of 57.17% (vehicle: 10.62 ± 1.78; dexamethasone: 16.69 ± 1.60; $p < 0.01$) and 31% (vehicle: 14.54 ± 2.08; dexamethasone: 19.04 ± 1.20; $p < 0.01$) at 6 and 10 months of age, respectively, in comparison with mice treated only with the vehicle (Fig. 4A, B). Interestingly, the basal density level of microglia is 37% higher at 10 months than 6 months of age ($p < 0.05$) and the effects of GRs agonist, as for the dendritic spine degeneration, are more prominent at 6 rather than 10 months of age ($p < 0.05$, Supplementary Fig. S1).

We further analysed microglia morphology and we found that, after dexamethasone treatment, both area and volume were significantly increased compared to vehicle alone at 6 and 10 months of age: the area was increased of 47.4% (vehicle: 3,45 μm^2 ± 785 μm^2; dexamethasone: 5084 μm^2 ± 618 μm^2; $p < 0.05$) and 59.3% (vehicle: 3773 μm^2 ± 715 μm^2; dexamethasone: 6008 μm^2 ± 324 μm^2; $p < .01$), respectively, while the volume was increased of 83.0% (vehicle: 804 μm^3 ± 270 μm^3; dexamethasone: 1471 ± 291; $p < 0.05$)

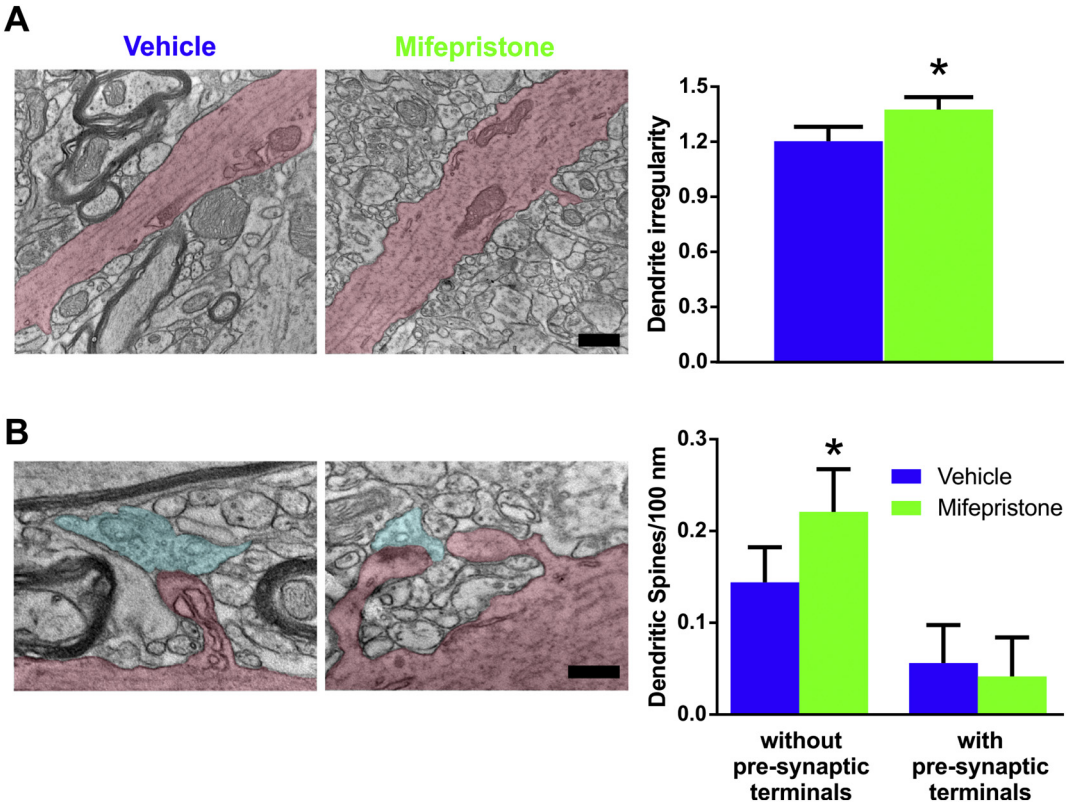

Fig. 2. Mifepristone increased dendritic irregularity and spine density. (A) Transmission electron micrographs of hippocampal CA1 dendrites of vehicle and mifepristone 3xTg-AD treated mice. The dendrites were digitally colored in pink in order to highlight the membrane profile. The bar graph shows the means ± (SD) of the index of dendritic membrane irregularity. (B) Transmission electron micrographs of hippocampal CA1 dendritic spines of control and mifepristone 3xTg-AD treated mice. The pre-synaptic terminal was digitally colored in azure and the post-synaptic element (dendritic spines) in pink. Note in the right the occurrence of a dendritic spine with a synaptic contact and a dendritic spine without pre-synaptic terminal. The bar graph shows the means ± (SD) of the dendritic spine densities. Significant differences are indicated as *p < .05. Scale bars = 200 nm (A) and 500 nm (B). (For interpretation of the references to colour in this figure legend, the reader is referred to the web version of this article.)

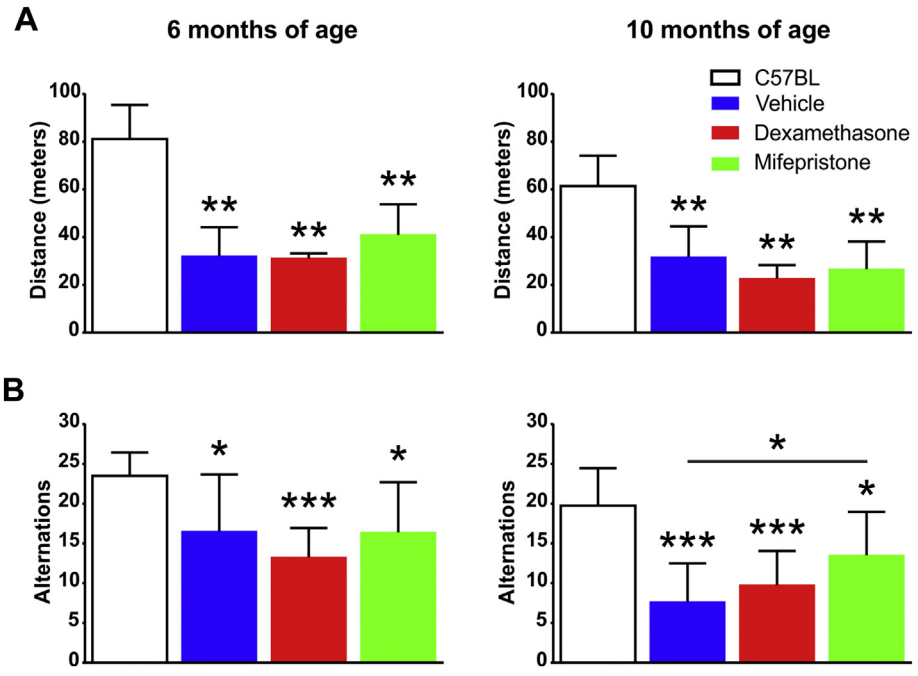

Fig. 3. GR modulation altered open field arena and y-maze test performance. (A) For Open Field it is reported the average distance, in meters, covered by every mice groups at 6 and 10 months of age. (B) For Y-maze task, it is reported the number of alternations reached by every groups. Significant differences are indicated as follows: *p < 0.05, **p < 0.01, ***p < 0.001.

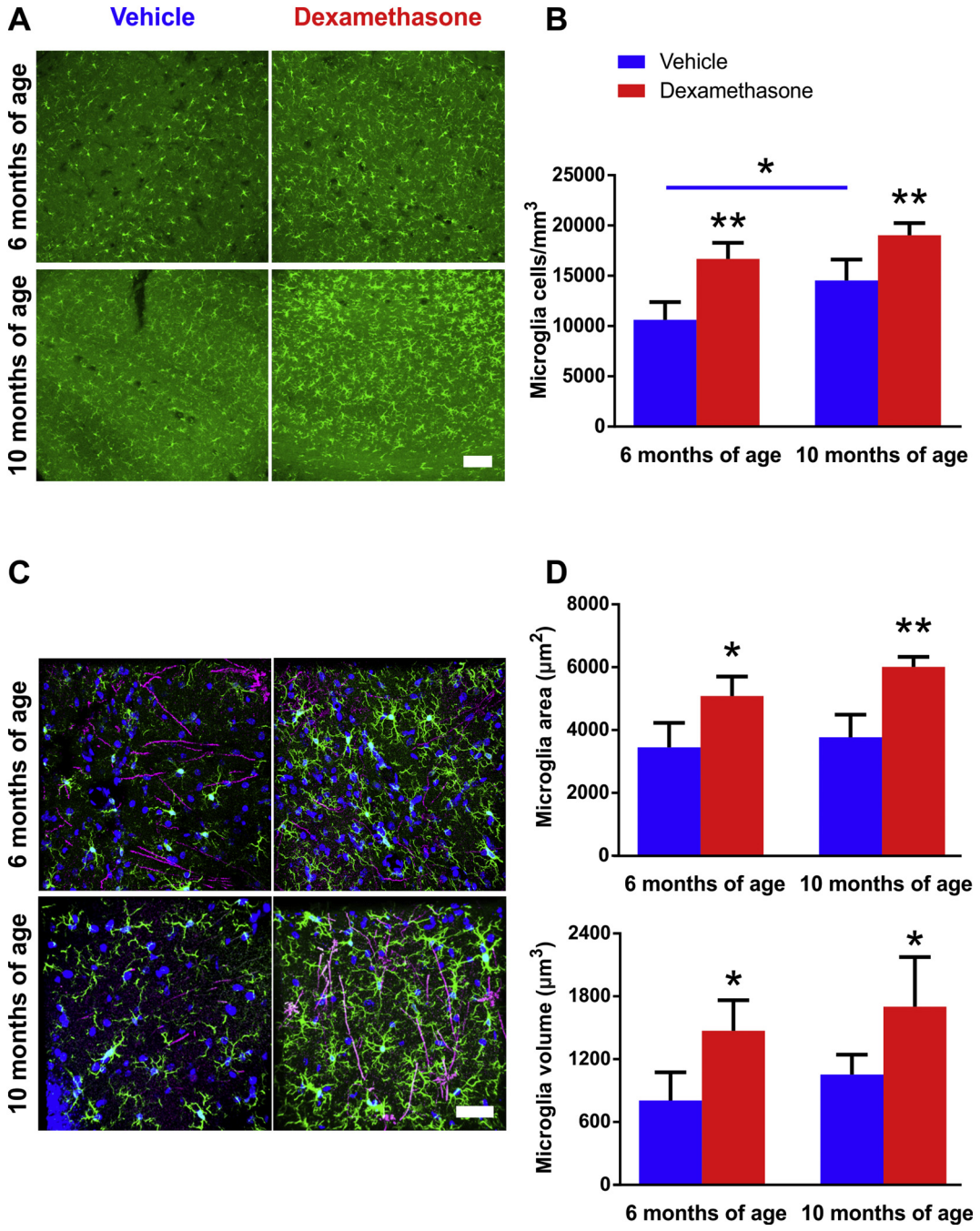

Fig. 4. Dexamethasone induced proliferation and activation of microglia in CA1 region of hippocampus of 3xTg-AD mice. (A) Confocal images of CA1 region of hippocampus of mice treated with dexamethasone or only vehicle. Microglia was marked (in green) using rabbit anti-IBA1 antibodies. (B) Bar graph of microglia density, both at 6 and 10 months of age. (C) Confocal images of CA1 region of hippocampus of mice treated with vehicle or dexamethasone. Microglia was marked (in green) using rabbit anti-IBA1 antibodies. Neurons (in purple) were visualized through reflective confocal microscopy. Nuclei are highlighted by DAPI in blue. (D) Bar graphs of area and volume of microglial cells at 6 and 10 months of age. Scale bars = 100 µm (A) and 40 µm (C). (For interpretation of the references to colour in this figure legend, the reader is referred to the web version of this article.)

and 61.5% (vehicle: 1054 ± 190; dexamethasone: 1702 ± 474; $p < 0.05$), respectively (Fig. 4C, D). Based on these results, in order to verify if the two main observations following dexamethasone treatment (drastic reduction of spine density and increased microglia activation) could be connected (Szepesi et al., 2018); we quantified the percentage of microglia in contact with neurons (defined as closer than 10 µm; Miyamoto et al., 2016) in vehicle-and dexamethasone-treated 3xTg-AD mice. A video of brain section stained with Golgi-Cox and with IBA1 (IF) is visible in the Supplementary Material. As shown in Fig. 5, in the vehicle group, 42.1 ± 9.8% and 44.5 ± 4.9% of the microglia signal was in contact with neurons, at 6 and 10 months of age, respectively (Fig. 5). Mice treated with the GRs agonist displayed significantly higher results: 53.4 ± 11.6% ($p < 0.001$) and 50.3 ± 11.3% ($p < 0.05$) at 6 and 10 months of age, respectively (Fig. 5). This trend is the same at distance less of 1 µm, but the difference between the two experimental group is not statistically significant (Fig. 5). Finally, we repeated the same experiments with the GRs antagonist mifepristone in 6 months old 3xTg-AD mice. We found that mifepristone produced a little reduction of microglia density (15.86%) in treated mice compared to the vehicle ($p < 0.05$), but no significative differences between

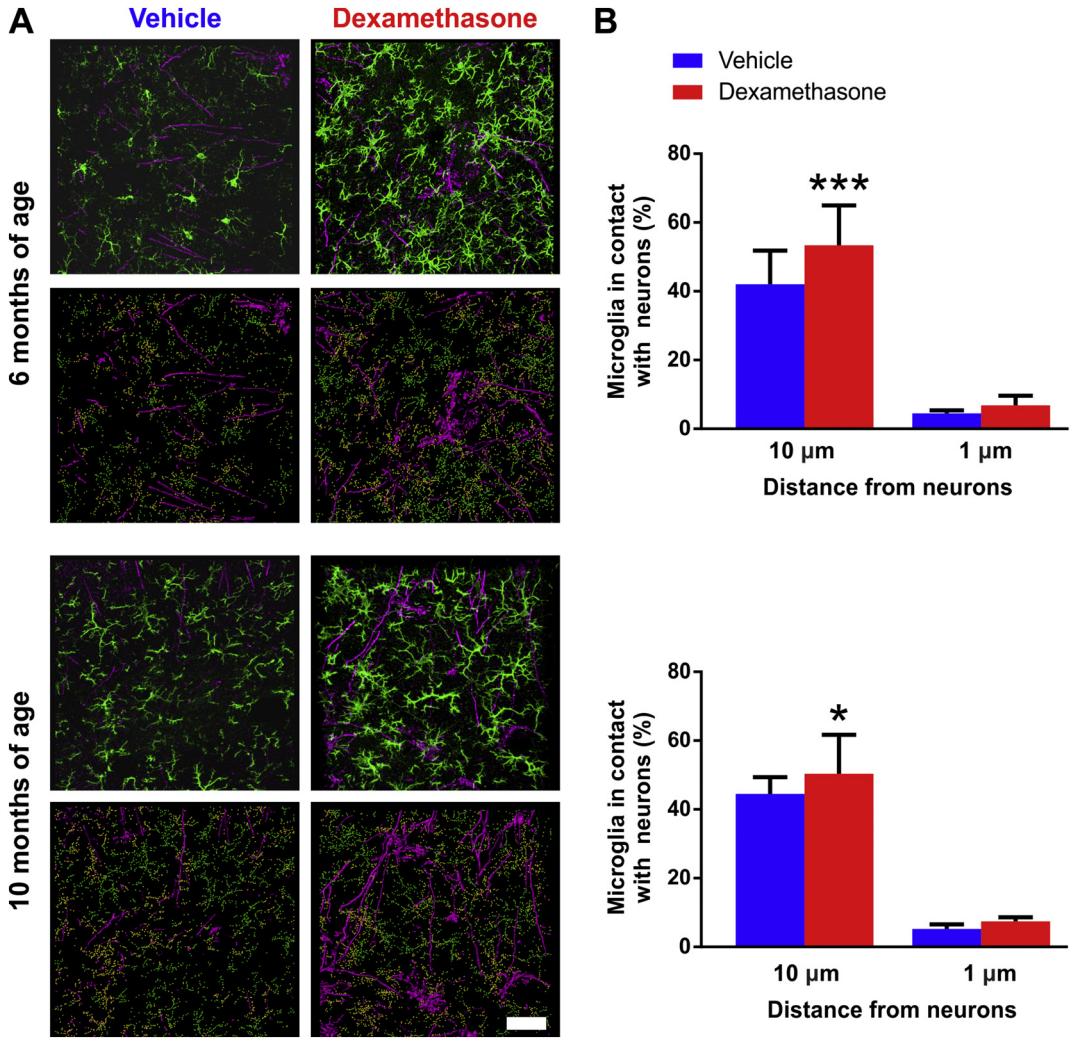

Fig. 5. Microglia-neuron interactions were increased in dexamethasone-treated 3xTg-AD mice. (A) Panel images for 6 and 10 months old 3xTg-AD mice. Microglia signal is visualized in green and neurons (Golgi) in magenta. Both raw signals (top) and reconstructed signals with Imaris (bottom) are shown. Yellow dots represent the percentage of microglia signal in contact with neurons. (B) Histograms of the mean percentage ± SD of microglia signal close to neurons, showing the untreated (vehicle) and treated (dexamethasone) mice groups in blue and red, respectively. Scale bar = 40 µm. (For interpretation of the references to colour in this figure legend, the reader is referred to the web version of this article.)

treated and control mice were found related to the area ($p = 0.28$) and the volume ($p = 0.55$, Supplementary Fig. S2).

3.4. High levels of grs modulators induced morphological and marker changes in microglia primary cultures

Previous papers demonstrated that microglial activation *in vitro* can be blocked by dexamethasone administration (Colton and Chernyshev, 1996; Drew and Chavis, 2000). To verify the effects of GRs agonist or antagonist on primary microglia, we treated microglial primary culture obtained from non-transgenic mice using 1 µM dexamethasone or 1 µM mifepristone or only vehicle for 4 h, as described in methods.

Unexpectedly, immunofluorescence experiments showed that dexamethasone treatment increased the signal of CD68, a marker of M1 phagocytic-pro inflammatory state of microglia (Fig. 6A). In addition, by WB and after dexamethasone treatment, CD68 was increased of about 209% ($p < 0.05$), while expression of CD206, a marker of M2 phagocytic-anti-inflammatory state, was not modulated ($p = 0.31$, Fig. 6B). Mifepristone treatment, instead, seemed to be able to activate both M1 and M2 phenotype. Immunoblotting, in every tested sample, showed an increase of CD68 and CD206, but the differences were not statistically significant, CD68 ($p = 0.26$) and CD206 ($p = 0.06$), likely to be due to the high variability of the obtained values.

Thus, our results, in contrast with previous published data, but in line with our *in vivo* results, showed that dexamethasone is able to activate a pro-inflammatory state of microglia *in vitro* through a direct mechanism.

4. Discussion

It has previously been shown that high circulating levels of GCs are able to increase the levels of Aβ and Tau proteins in 3xTg-AD mice (Green et al., 2006). Our results show that GCs promote also a premature loss of dendritic spine density in CA1 region of the hippocampus of 3xTg-AD mice before the appearance of the plaques (Belfiore et al., 2019; Oddo et al., 2003). Moreover, GCs strongly increased the density and the activation of microglia in CA1 region of the hippocampus. In contrast, mifepristone increases the spine density and improves the behavioural performance of treated animals.

Dendritic spines are plastic structures and their dynamic changes have important implications for learning and memory processes in the mammalian brain (Sala and Segal, 2014). Loss of dendritic spines has been described in post-mortem studies in early-to-mild AD patients and in age-dependent manner in several animal models of AD (Bolognin

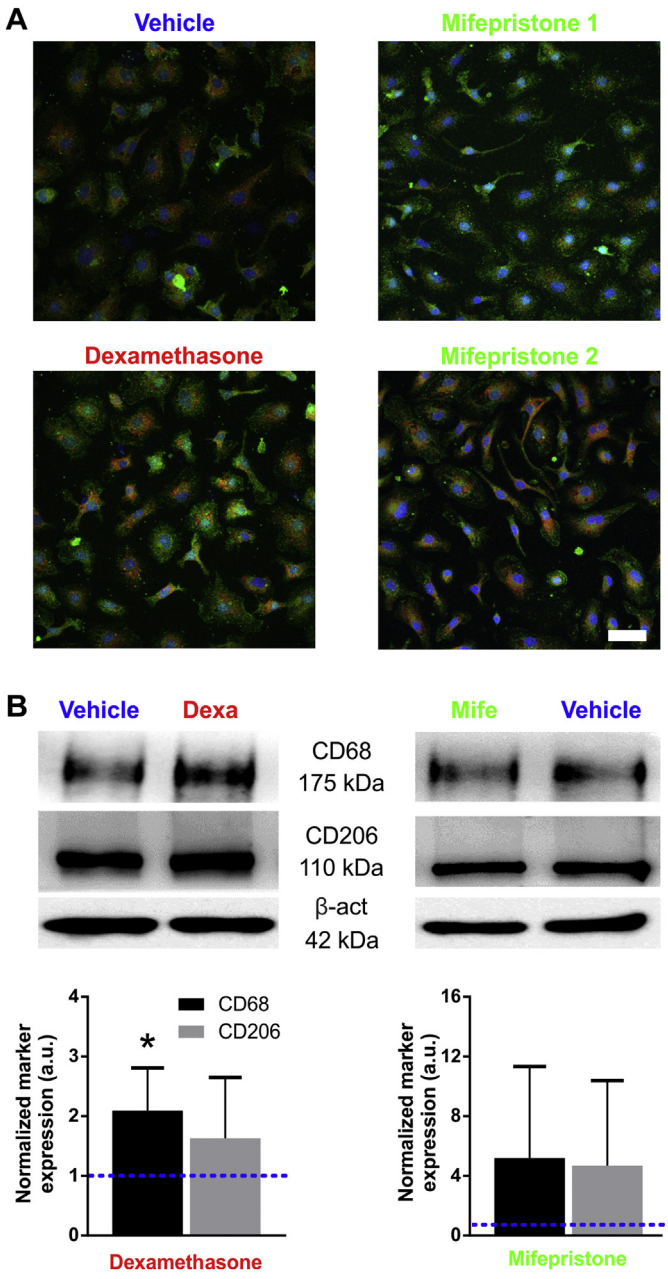

Fig. 6. GR agonist and antagonist changed the morphology and activity of primary microglia in culture. (A) Confocal images of primary microglia culture treated with vehicle or 1 μM of dexamethasone or 1 μM of mifepristone and stained with anti-CD68 (red), anti-IBA1 (green) and DAPI (blue). (B) Immunoblotting of primary microglia culture treated with vehicle or 1 μM of dexamethasone or 1 μM of mifepristone. Significant differences are indicated as *$p < 0.05$. Scale bar = 40 μm. (For interpretation of the references to colour in this figure legend, the reader is referred to the web version of this article.)

et al., 2014). In 3xTg-AD mice dendritic spine degeneration becomes evident during the last stage of the disease and after Aβ plaque appearance (Bittner et al., 2010). The mechanisms underlying the spine loss in 3xTg-AD mice after treatment with GCs at 6 and 10 months could be linked to an increase of Aβ and to an excessive activation of microglia by GCs, and finally to a mechanism involving the gene transcription regulation promoted by GRs and MRs.

Although *in vitro* studies demonstrate that cortisone and GRs agonists were able to exert anti-inflammatory effects on microglial cells (Colton and Chernyshev, 1996; Drew and Chavis, 2000), several lines of evidence show *in vivo* pro-inflammatory effects of GCs (Duque Ede and Munhoz, 2016; Munhoz et al., 2006; Munhoz et al., 2010; Nair and Bonneau, 2006; Sorrells et al., 2009). Indeed, prolonged exposition to GCs enhances the inflammation response to specific stimuli, such as lipopolysaccharide or kainic acid, in brain (Duque Ede and Munhoz, 2016; Sorrells et al., 2009). This GCs priming effect is time and region-dependent (Duque Ede and Munhoz, 2016; Munhoz et al., 2010). The enhance of inflammation involved the activation of microglia and neuron signals (Frank et al., 2014; Nair and Bonneau, 2006; van Olst et al., 2018). Indeed, Sorrells et al. have shown that the treatment with minocycline, an inhibitor of microglial activation, reduces the neuronal damage after stereotaxic injection in the brain of kainic acid, suggesting an important role of microglia activity (Sorrells et al., 2014). Instead, Nair and Bonneau have shown that activation of microglia by GCs in C57BL/6 mice is not directly promoted by GRs activation on microglia, but it is mediated by a neuron-dependent mechanism, involving NMDA receptor hyper-activation (Nair and Bonneau, 2006). Unexpectedly, our results on microglia have shown that dexamethasone is able to activate microglia not only *in vivo* in CA1 region of hippocampus of 3xTg-AD mice, but also *in vitro* primary cell culture. The discrepancy between our results and the data in literature could be explained by the well-known biphasic effects of glucocorticoids in brain, a phenomenon called Hormesis (Lupien et al., 2005). Several physiological molecules are likely to show a hormetic effect with opposite effects depending on high or low concentrations (Puzzo et al., 2012). For GCs the biphasic behaviour seems to be more complex: it is linked not only to the concentration of the hormone but also to the time of exposure (acute or chronic)(Sorrells et al., 2009). In regard to spines, we observed that high and chronic circulating levels of GRs agonist disrupt the spine turnover promoting their premature degeneration. On the contrary, we know from literature that acute or low dosage of GCs promotes spine turnover in brain (Liston and Gan, 2011). In regard to activation of microglia *in vitro* induced by dexamethasone, this effect could be related to doses and time of treatment in our conditions. Thus, while the microglia activation observed *in vitro* shows a direct mechanism of GCs on microglia cells, our *in vivo* experiments are not able to confirm or exclude a direct mechanism in 3xTg-AD after GCs treatment. This aspect will be studied in detail in future experiments.

It is already well known that mifepristone can reduce amyloid plaques in 3xTg-AD mice and in other AD mouse models (Baglietto-Vargas et al., 2013; Pineau et al., 2016). Here, we found, by Golgi-Cox staining, that mifepristone treatment also promoted spine formations in CA1 region of hippocampus in 3xTg-AD mice, both at 6 and 10 months of age. These effects were confirmed by electron microscopy (EM) at 6 months of age. Moreover, we observed a marked irregularity of dendrites in 3xTg-AD mice treated with mifepristone, that could be related to the process of formation of new spines. Lastly, we would like to highlight the presence of some perforated synapses, indicative of synaptic plasticity, in mifepristone treated 3xTg-AD mice compared to vehicle treated animals, in which we had not found any (Bertoni-Freddari et al., 2008; Stewart et al., 2005). Thus, mifepristone can partially revert the loss of spines that could be translated in an improvement of the cognitive performance observed by the Y-maze task at 10 months of age.

The effects of mifepristone on microglia were instead unclear. In particular, *in vivo* experiments, mifepristone slightly reduced microglia density at 6 months of age but had no effect on its morphology. Surprisingly, in *in vitro* experiments, microglia after treatment with mifepristone showed an increase of both CD68, a marker of M1 pro-inflammatory microglia, and CD206, a marker of M2 anti-inflammatory microglia, in every trial but with a high variability. Unfortunately, we do not have an explanation for these results, but we speculate that the phenomenon could be explained by the heterogeneity of microglia cultures (Li et al., 2019).

It is noteworthy to observe that the negative effects produced by dexamethasone-induced stress is prominent at the beginning of AD rather than at the medium late phase of AD, as we demonstrated both

for dendritic spine degeneration and microglia activation. These data are in line with the clinical observations: a) in AD patients, cognitive and psychological symptoms are associated with an early deregulation of the HPA axis; b) in healthy and elderly individuals with high cortisol levels were significantly more likely to develop AD; and c) in AD patients, high levels of cortisol in the plasma and in the cerebrospinal fluid have been associated with a rapid and severe cognitive decline (Ouanes and Popp, 2019). Therefore, the stronger effects observed at 6 months of age compared to 10 months of age in 3xTg-AD mice could be correlated to the prominent role of stressful life events in the preclinical stages of AD in human.

In conclusion, our data support the existence of a strong relationship between AD and GCs. Stress is a key risk factor for the beginning and the rapidity progression of the disease of AD, as demonstrated by our dexamethasone treatment of the transgenic mouse model of AD, the 3xTg-AD mouse. A similar correlation between high circulating levels of GCs and the risk of AD development was found also in human (Pietrzak et al., 2017; Wilson et al., 2005). Moreover, our results show that the treatment with antagonist of GRs is able to stimulate synaptic plasticity, implement cognitive abilities and behavioural performance and partially decrease the general state of inflammation in the brain. Consequently, the reduction of stress, promoted by suppression of GRs activity, could represent a promising therapeutic strategy to postpone the onset of AD and slow down its progression. However, the biphasic behaviour of GCs requires an in-depth study to understand the ideal dosage and timing for the treatment. It is important to emphasize that the treatment with mifepristone in AD patients slows the cognitive decline, but induces side effects, such as an increase of the blood levels of GCs (Canet et al., 2018). Some specific GRs antagonists, with lower side effects, have recently been developed, but they have not yet been tested (Canet et al., 2018). Thus, our results and the literature data strongly support the need to continue these studies in order to collect further data for a possible transition to the clinical research.

Supplementary data to this article can be found online at https://doi.org/10.1016/j.nbd.2019.104568.

Author contributions

MP and MB designed the experiments. MP carried out the Golgi staining, the IF and the analysis of the images. LJ contributed to the image analysis. ML performed the immunoblotting and the analysis. BC and MMa performed the electron microscopy. GP and AS performed the behaviour analysis. MP, MMe and MB wrote the manuscript. All authors reviewed and approved the final manuscript.

Declaration of Competing Interest

The authors declare no competing financial interests.

Acknowledgments

This work was supported from University of Verona, Joint Project-JPVR173ZR8. We thank the Centro Piattaforme Tecnologiche-University of Verona to give us access to the imaging platform. We thank Professor G. Constantin and the members of her laboratory for their invaluable help in the behavior analyses. We thank the students M. Antolini, F. Marchiotto, B. Rossato and C. Barbagallo for their help with the IF and Golgi staining and the research fellow A. Avesani for her help with the WB.

References

Baglietto-Vargas, D., et al., 2013. Mifepristone alters amyloid precursor protein processing to preclude amyloid beta and also reduces tau pathology. Biol. Psychiatry 74, 357–366.
Belfiore, R., et al., 2019. Temporal and regional progression of Alzheimer's disease-like pathology in 3xTg-AD mice. Aging Cell 18, e12873.
Bertoni-Freddari, C., et al., 2008. Decreased presence of perforated synapses in a triple-transgenic mouse model of Alzheimer's disease. Rejuvenation Res. 11, 309–313.
Bisht, K., et al., 2018. Chronic stress as a risk factor for Alzheimer's disease: roles of microglia-mediated synaptic remodeling, inflammation, and oxidative stress. Neurobiol. Stress 9, 9–21.
Bittner, T., et al., 2010. Multiple events lead to dendritic spine loss in triple transgenic Alzheimer's disease mice. PLoS One 5, e15477.
Bolognin, S., et al., 2014. The potential role of rho GTPases in Alzheimer's disease pathogenesis. Mol. Neurobiol. 50, 406–422.
Borin, M., et al., 2018. Rac1 activation links tau hyperphosphorylation and Abeta dysmetabolism in Alzheimer's disease. Acta Neuropathol. Commun. 6, 61.
Canet, G., et al., 2018. Central role of glucocorticoid receptors in Alzheimer's disease and depression. Front. Neurosci. 12, 739.
Carroll, J.C., et al., 2011. Chronic stress exacerbates tau pathology, neurodegeneration, and cognitive performance through a corticotropin-releasing factor receptor-dependent mechanism in a transgenic mouse model of tauopathy. J. Neurosci. 31, 14436–14449.
Colton, C.A., Chernyshev, O.N., 1996. Inhibition of microglial superoxide anion production by isoproterenol and dexamethasone. Neurochem. Int. 29, 43–53.
Csernansky, J.G., et al., 2006. Plasma cortisol and progression of dementia in subjects with Alzheimer-type dementia. Am. J. Psychiatry 163, 2164–2169.
Das, G., et al., 2013. The Golgi-cox method. Methods Mol. Biol. 1018, 313–321.
de Quervain, D.J., et al., 2004. Glucocorticoid-related genetic susceptibility for Alzheimer's disease. Hum. Mol. Genet. 13, 47–52.
De Strooper, B., Karran, E., 2016. The cellular phase of Alzheimer's disease. Cell 164, 603–615.
Dienes, K.A., et al., 2013. Cortisol secretion in depressed, and at-risk adults. Psychoneuroendocrinology 38, 927–940.
Dong, H., et al., 2008. Corticosterone and related receptor expression are associated with increased beta-amyloid plaques in isolated Tg2576 mice. Neuroscience 155, 154–163.
Dorostkar, M.M., et al., 2015. Analyzing dendritic spine pathology in Alzheimer's disease: problems and opportunities. Acta Neuropathol. 130, 1–19.
Drew, P.D., Chavis, J.A., 2000. Inhibition of microglial cell activation by cortisol. Brain Res. Bull. 52, 391–396.
Duque Ede, A., Munhoz, C.D., 2016. The pro-inflammatory effects of glucocorticoids in the brain. Front Endocrinol. (Lausanne) 7, 78.
Ferreira, S.T., et al., 2015. Soluble amyloid-beta oligomers as synaptotoxins leading to cognitive impairment in Alzheimer's disease. Front. Cell. Neurosci. 9, 191.
Finsterwald, C., Alberini, C.M., 2014. Stress and glucocorticoid receptor-dependent mechanisms in long-term memory: from adaptive responses to psychopathologies. Neurobiol. Learn. Mem. 112, 17–29.
Frank, M.G., et al., 2014. Chronic exposure to exogenous glucocorticoids primes microglia to pro-inflammatory stimuli and induces NLRP3 mRNA in the hippocampus. Psychoneuroendocrinology 40, 191–200.
Gibb, R., Kolb, B., 1998. A method for vibratome sectioning of Golgi-cox stained whole rat brain. J. Neurosci. Methods 79, 1–4.
Green, K.N., et al., 2006. Glucocorticoids increase amyloid-beta and tau pathology in a mouse model of Alzheimer's disease. J. Neurosci. 26, 9047–9056.
Hammar, A., Ardal, G., 2009. Cognitive functioning in major depression–a summary. Front. Hum. Neurosci. 3, 26.
Joshi, Y.B., et al., 2012. Stress hormone leads to memory deficits and altered tau phosphorylation in a model of Alzheimer's disease. J. Alzheimers Dis. 31, 167–176.
Kootar, S., et al., 2018. Identification of an acute functional cross-talk between amyloid-beta and glucocorticoid receptors at hippocampal excitatory synapses. Neurobiol. Dis. 118, 117–128.
Lante, F., et al., 2015. Subchronic glucocorticoid receptor inhibition rescues early episodic memory and synaptic plasticity deficits in a mouse model of Alzheimer's disease. Neuropsychopharmacology 40, 1772–1781.
Lemaire, V., et al., 2000. Prenatal stress produces learning deficits associated with an inhibition of neurogenesis in the hippocampus. Proc. Natl. Acad. Sci. U. S. A. 97, 11032–11037.
Li, Q., et al., 2019. Developmental heterogeneity of microglia and brain myeloid cells revealed by deep single-cell RNA sequencing. Neuron 101, 207–223 (e10).
Liston, C., Gan, W.B., 2011. Glucocorticoids are critical regulators of dendritic spine development and plasticity in vivo. Proc. Natl. Acad. Sci. U. S. A. 108, 16074–16079.
Lupien, S.J., et al., 2005. Hormetic influence of glucocorticoids on human memory. Nonlinearity Biol. Toxicol. Med. 3, 23–56.
Magarinos, A.M., et al., 1996. Chronic psychosocial stress causes apical dendritic atrophy of hippocampal CA3 pyramidal neurons in subordinate tree shrews. J. Neurosci. 16, 3534–3540.
Mcquade, A., Blurton-Jones, M., 2019. Microglia in Alzheimer's disease: exploring how genetics and phenotype influence risk. J. Mol. Biol. 431, 1805–1817.
Mirescu, C., et al., 2006. Sleep deprivation inhibits adult neurogenesis in the hippocampus by elevating glucocorticoids. Proc. Natl. Acad. Sci. U. S. A. 103, 19170–19175.
Miyamoto, A., et al., 2016. Microglia contact induces synapse formation in developing somatosensory cortex. Nat. Commun. 7, 12540.
Munhoz, C.D., et al., 2006. Chronic unpredictable stress exacerbates lipopolysaccharide-induced activation of nuclear factor-kappaB in the frontal cortex and hippocampus via glucocorticoid secretion. J. Neurosci. 26, 3813–3820.
Munhoz, C.D., et al., 2010. Glucocorticoids exacerbate lipopolysaccharide-induced signaling in the frontal cortex and hippocampus in a dose-dependent manner. J. Neurosci. 30, 13690–13698.
Nair, A., Bonneau, R.H., 2006. Stress-induced elevation of glucocorticoids increases

microglia proliferation through NMDA receptor activation. J. Neuroimmunol. 171, 72–85.
Oddo, S., et al., 2003. Triple-transgenic model of Alzheimer's disease with plaques and tangles: intracellular Abeta and synaptic dysfunction. Neuron 39, 409–421.
Ouanes, S., Popp, J., 2019. High cortisol and the risk of dementia and Alzheimer's disease: a review of the literature. Front. Aging Neurosci. 11, 43.
Paolicelli, R.C., Ferretti, M.T., 2017. Function and dysfunction of microglia during brain development: consequences for synapses and neural circuits. Front Synaptic Neurosci. 9, 9.
Pietrzak, R.H., et al., 2017. Plasma cortisol, brain amyloid-beta, and cognitive decline in preclinical Alzheimer's disease: a 6-year prospective cohort study. Biol. Psychiatry Cogn. Neurosci. Neuroimaging 2, 45–52.
Piirainen, S., et al., 2017. Psychosocial stress on neuroinflammation and cognitive dysfunctions in Alzheimer's disease: the emerging role for microglia? Neurosci. Biobehav. Rev. 77, 148–164.
Pineau, F., et al., 2016. New selective glucocorticoid receptor modulators reverse amyloid-beta peptide-induced hippocampus toxicity. Neurobiol. Aging 45, 109–122.
Puzzo, D., et al., 2012. Hormetic effect of amyloid-beta peptide in synaptic plasticity and memory. Neurobiol. Aging 33 (1484), e15–e24.
Sala, C., Segal, M., 2014. Dendritic spines: the locus of structural and functional plasticity. Physiol. Rev. 94, 141–188.
Scheff, S.W., et al., 2007. Synaptic alterations in CA1 in mild Alzheimer disease and mild cognitive impairment. Neurology 68, 1501–1508.
Serrano-Pozo, A., et al., 2011. Neuropathological alterations in Alzheimer disease. Cold Spring Harb. Perspect. Med. 1, a006189.
Sierra, A., et al., 2008. Steroid hormone receptor expression and function in microglia. Glia 56, 659–674.
Sorrells, S.F., et al., 2009. The stressed CNS: when glucocorticoids aggravate inflammation. Neuron 64, 33–39.
Sorrells, S.F., et al., 2014. Glucocorticoids increase excitotoxic injury and inflammation in the hippocampus of adult male rats. Neuroendocrinology 100, 129–140.
Spiga, S., et al., 2011. Simultaneous Golgi-cox and immunofluorescence using confocal microscopy. Brain Struct. Funct. 216, 171–182.
Stewart, M.G., et al., 2005. Chemically induced long-term potentiation increases the number of perforated and complex postsynaptic densities but does not alter dendritic spine volume in CA1 of adult mouse hippocampal slices. Eur. J. Neurosci. 21, 3368–3378.
Swaab, D.F., et al., 1994. Increased cortisol levels in aging and Alzheimer's disease in postmortem cerebrospinal fluid. J. Neuroendocrinol. 6, 681–687.
Szepesi, Z., et al., 2018. Bidirectional microglia-neuron communication in health and disease. Front. Cell. Neurosci. 12, 323.
Umegaki, H., et al., 2000. Plasma cortisol levels in elderly female subjects with Alzheimer's disease: a cross-sectional and longitudinal study. Brain Res. 881, 241–243.
van Olst, L., et al., 2018. Glucocorticoid-mediated modulation of morphological changes associated with aging in microglia. Aging Cell 17, e12790.
Wang, S., Colonna, M., 2019. Microglia in Alzheimer's disease: a target for immunotherapy. J. Leukoc. Biol. 106, 219–227.
Wilson, R.S., et al., 2005. Proneness to psychological distress and risk of Alzheimer disease in a biracial community. Neurology. 64, 380–382.
Wirths, O., Bayer, T.A., 2010. Neuron loss in transgenic mouse models of Alzheimer's disease. Int. J. Alzheimers Dis. 2010.
Zaqout, S., Kaindl, A.M., 2016. Golgi-cox staining step by step. Front. Neuroanat. 10, 38.
Ziegler-Waldkirch, S., Meyer-Luehmann, M., 2018. The role of glial cells and synapse loss in mouse models of Alzheimer's disease. Front. Cell. Neurosci. 12, 473.